Bioorganic & Medicinal Chemistry Letters 21 (2011) 5778–5783

Contents lists available at SciVerse ScienceDirect

Bioorganic & Medicinal Chemistry Letters

journal homepage: www.elsevier.com/locate/bmcl

Lead generation of heat shock protein 90 inhibitors by a combination of fragment-based approach, virtual screening, and structure-based drug design

Takaaki Miura [a,*], Takaaki A. Fukami [a], Kiyoshi Hasegawa [a], Naomi Ono [a], Atsushi Suda [a], Hidetoshi Shindo [a], Dong-Oh Yoon [b], Sung-Jin Kim [b], Young-Jun Na [b], Yuko Aoki [a], Nobuo Shimma [a], Takuo Tsukuda [a], Yasuhiko Shiratori [a]

[a] Kamakura Research Laboratories, Chugai Pharmaceutical Co., Ltd, 200 Kajiwara, Kamakura, Kanagawa 247-8530, Japan
[b] C&C Research Laboratories, 146-141 Annyeong-dong, Hwaseong-si, Gyeonggi-do 445-380, Republic of Korea

ARTICLE INFO

Article history:
Received 4 June 2011
Revised 29 July 2011
Accepted 1 August 2011
Available online 6 August 2011

Keywords:
Virtual screening
Fragment-based approach
Hsp90 inhibitor

ABSTRACT

Heat shock protein 90 (Hsp90) is a molecular chaperone which regulates maturation and stabilization of its substrate proteins, known as client proteins. Many client proteins of Hsp90 are involved in tumor progression and survival and therefore Hsp90 can be a good target for developing anticancer drugs. With the aim of efficiently identifying a new class of orally available inhibitors of the ATP binding site of this protein, we conducted fragment screening and virtual screening in parallel against Hsp90. This approach quickly identified 2-aminotriazine and 2-aminopyrimidine derivatives as specific ligands to Hsp90 with high ligand efficiency. In silico evaluation of the 3D X-ray Hsp90 complex structures of the identified hits allowed us to promptly design CH5015765, which showed high affinity for Hsp90 and antitumor activity in a human cancer xenograft mouse model.

The 90-kDa heat shock proteins (Hsp90) are ATP-dependent molecular chaperones which are responsible for the stabilization and maturation of their substrate proteins, known as client proteins.[1] The client proteins of Hsp90 include many oncology targets such as p53 mutants, Raf1, Akt, and Bcr-Abl, which are important for tumor generation and progression. Therefore, an inhibition of Hsp90 could lead to an effective suppression of tumors by interfering with multiple oncogenic pathways simultaneously. Although there once was concern about the adverse effect of a ubiquitous expression of Hsp90 in both normal and tumor cells, it has since been shown that a selective suppression of tumor cells was indeed achievable with the discovery of selective Hsp90 inhibitors, geldanamycin and radicicol.[2] When geldanamycin derivatives, 17AAG and 17DMAG, subsequently proceeded to clinical trials, it stimulated the community to make significant efforts to discover and develop a different class of Hsp90 inhibitors with better DMPK profiles and antitumor activities.[1,3]

In this report, we describe our attempt to generate a new class of orally available Hsp90 inhibitors by a combinatorial approach of fragment screening, virtual screening and molecular modeling with the assistance of X-ray structures of Hsp90–ligand complexes. Several groups have reported the discovery of Hsp90 inhibitors by virtual screening or fragment screening.[4,5] Also, the combination of fragment and virtual screening for Hsp90 inhibitor generation was recently reported.[6] In this study, we adopted the parallel approach of fragment and virtual screening and the information obtained from the two approaches was utilized directly with the aim of generating inhibitors more efficiently and effectively. In fragment screening, only a small set of fragments selected for targeting the ATP binding site was screened, and the potentially limited chemical space when searching in the fragment screening was compensated for by conducting virtual screening, which explored for wider chemical space. The binding of small molecule ligands to Hsp90 can be characterized by two important interactions[7,8]: (1) the hydrogen bonding network mediated by the carboxylic side chain of Asp93 and crystal waters; (2) two hydrophobic pockets formed by Leu107-Phe138 and Ile96. Notably, the hydrogen bonding network involving Asp93 and associated crystal waters is conserved for all ATP site binders (Fig. 1). Thus, our strategy was to first exploit the Asp93 site in the fragment and virtual screening to identify initial binders and then, with the help of the X-ray structures of Hsp90-inhibitor complexes, to design new inhibitors based on the identified hits to gain additional interaction with the protein.

In humans, two isoforms of Hsp90, namely, Hsp90 α and β, are known. In this study, the N-terminal domain (9–237) of human Hsp90α was used for all biophysical analysis. The domain was expressed in *Escherichia coli*, and purified to homogeneity by standard column chromatography. For ATPase assay, full-length HSP90α expressed as N-terminally GST-tagged form in *E. coli*, was employed. The issue with the ATPase assay was its inherent low sensitivity caused by the weak Hsp90 ATPase activity.

* Corresponding author. Tel.: +81 467 47 6019; fax: +81 467 45 6824.
E-mail address: miuratka@chugai-pharm.co.jp (T. Miura).

0960-894X/$ - see front matter © 2011 Elsevier Ltd. All rights reserved.
doi:10.1016/j.bmcl.2011.08.001

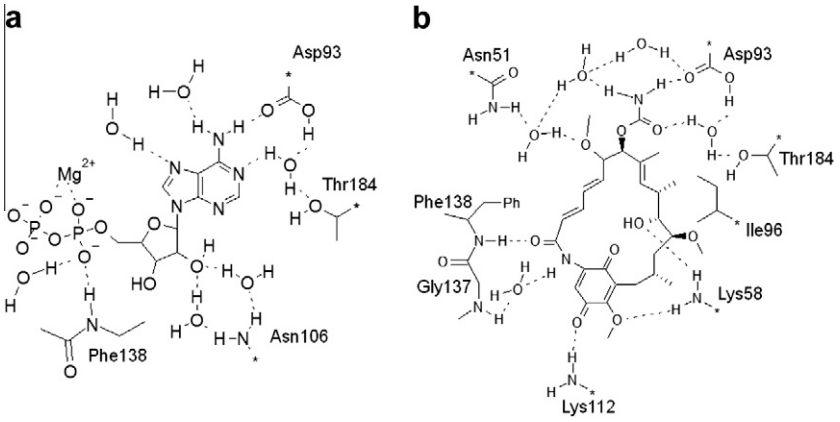

Figure 1. Schematic drawing of the interaction between Hsp90α and ADP (a) and geldanamycin (b).

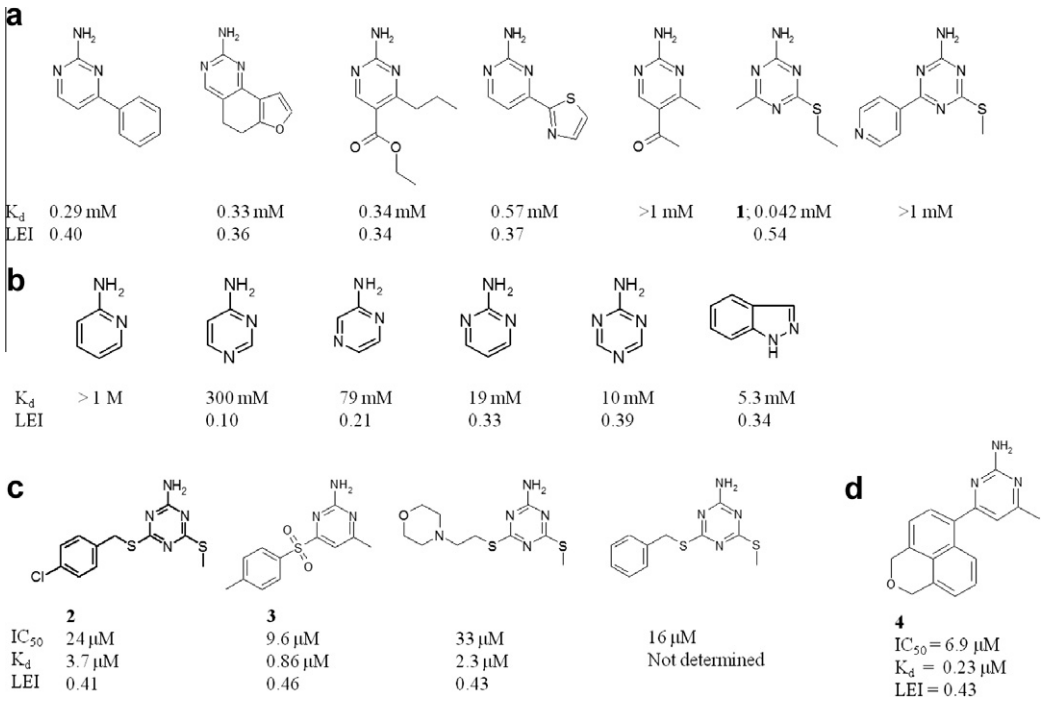

Figure 2. Chemical structures of representative hits. (a) Fragment hits; (b) 2-aminopyrimidine and its analogues; (c) hit compounds from hit expansion of fragment hits; (d) hit compound from virtual screening. K_d, LEI, and IC_{50} values are shown together with chemical structure when available. LEI was calculated using the equation, LEI = ΔG/(no. of heavy atoms).[12]

In fragment screening, surface Plasmon resonance (SPR)-based binding assay was employed to screen 164 purchased fragments which possess a donor–acceptor pattern complimentary to the hydrogen bonding network of the Asp93 site. A highly active and stable surface of Hsp90 was prepared by coupling minimally biotinylated Hsp90 to the streptavidine-coated surface of a sensor chip (type SA, GE healthcare) (Supplementary Fig. 1). Nineteen compounds were classified as active, showing more than 50% occupancy of the immobilized Hsp90 at the screening concentration of 250 μM. Reproducibility and dose dependence of the binding response narrowed down these 19 initial hits to 13 compounds. Then, these 13 fragments were subjected to two different types of NMR experiments to verify that they bound to the ATP pocket of Hsp90. The first were 1D ^{1}H displacement experiments that examined if the addition of geldanamycin suppressed the line-broadening of proton signals of a test fragment induced by binding to Hsp90 (Supplementary Fig. 2).[9] The second were 2D ^{1}H–^{15}N-HSQC chemical shift perturbation experiment in which determining the chemical shift difference experienced by the HN-group of each amino acid allowed us to map the binding sites of the fragment hits (Supplementary Fig. 3).[10] The analysis indicated that all 13 fragments did indeed bind to the designated active site of the protein. Interestingly, 8 out of 13 validated fragment hits possess 2-aminopyrimidine and 2-aminotriazine as core motifs, as shown in Figure 2a. This finding prompted us to determine the affinities of 2-aminotriazine and its analogues for Hsp90 so as to prioritize them as a core motif for hit expansion by substructure search. The dissociation constants of the compounds were determined by recording a series of 2D NMR NH-correlation spectra at various concentrations of the test fragment and by following the size of chemical shift changes of NH crosspeaks (Fig. 2b). The result indicated that 2-aminopyrimidine, 2-aminotriazine and indazole

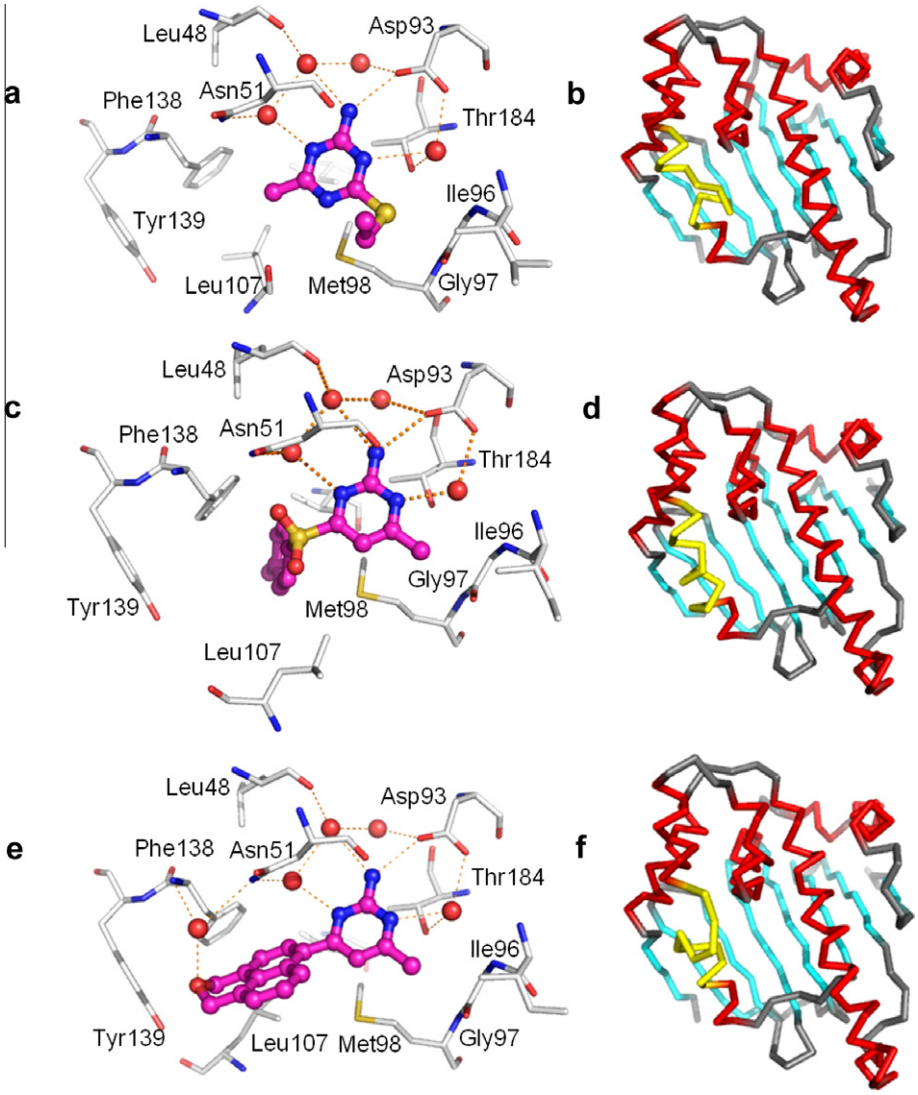

Figure 3. X-ray structures of N-terminal Hsp90α in complex with identified compounds. Detailed binding mode of the active site and the overall structure are shown. The overall structures are colored according to the secondary structure with α-helices in red and β-strands in cyan. The flexible loops consisting of residues 108–112, are colored in yellow. (a and b) Fragment hit, **1**; (c and d) fragment hit, **3**; (e and f) a hit from virtual screening, **4**.

showed better affinity among those tested. Therefore, we collected from our in-house library, 710 compounds possessing these moieties as the core structures. These compounds were screened using the ATPase assay with full-length Hsp90α[11] instead of SPR because of a higher throughput of the ATPase assay. Notably, 16 compounds showed IC_{50} values less than 100 μM with the most potent compounds, **2** and **3**, having IC_{50} values of 24 and 9.6 μM, respectively (Fig. 2c). Calculation of ligand efficiency index[12] (LEI = $-\Delta G$/(the number of heavy atoms in the ligand)) for fragment hits and active compounds from the hit expansion indicated that good ligand efficiency was maintained for the hits from the expansion, although the highest LEI was found for a hit fragment, **1**, with a LEI of 0.54.

Our second approach for identifying Hsp90 inhibitors was virtual screening using a docking tool, FlexX.[13] From an in-house source, 435,000 compounds were used to dock for the screening. The program CORINA[14] was employed to convert these compounds in the docking library from 2D to 3D and the complex structure between Hsp90 and geldanamycin (PDB entry: 1YET) was used as a template. The active site was defined as a sphere consisting of the atoms within 10 Å from geldanamycin. In addition, three water molecules around the carboxylic group of Asp93 were also included as a part of the binding site, as these three water molecules were consistently found in the X-ray structures of Hsp90 in complex with small molecules binding to the ATP site. Following the docking by FlexX, the 3000 highest-scoring compounds were selected for further analysis and each compound was visually inspected on the graphics as to whether they bound to the Asp93 site as designated and/or were chemically tractable. After this filtering process, 1460 compounds remained and were tested for their inhibitory activity against Hsp90α by ATPase assay at 100 μM.[11] Seventy-three compounds showed an inhibitory activity larger than 30% and an outstanding activity was observed for compound **4** with an IC_{50} value of 6.9 μM and LEI of 0.43 (Fig. 2d).

In order to obtain detailed structural information on the binding mode of the compounds, crystallization was performed[15] and the X-ray crystal structures of the complex with Hsp90 were solved for **1**, **3**, and **4**.[16] As expected, the 2-aminopyrimidine and triazine moieties of these compounds are accommodated in the Asp93 site in the same manner but also differences were found among these structures in the conformation of residues Ile110-Gly114. This part consists of a central portion of a long α-helix in the structure of **3**,

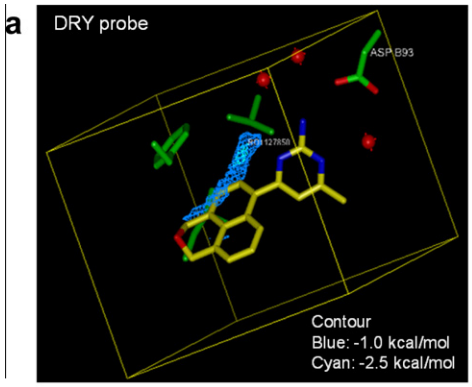

b

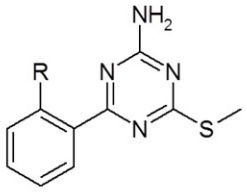

	5; R = H	6; R=CH_3	7; R = Cl
Hsp90α IC_{50} (μM):	31	0.57	0.75
K_d (μM):	51	4.5	6.9
LEI:	0.39	0.45	0.44
HCT116 IC_{50} (μM):	>100	47	94

c

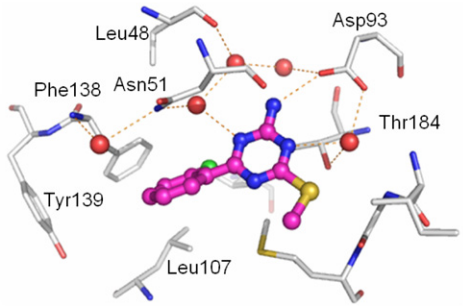

Figure 4. Detailed analyses of compound **4**. (a) The GRID analysis for compound **4**. The location of DRY probe is shown in cyan. (b) SAR to evaluate the effect of the *ortho*-substitution at the left phenyl ring. (c) Detailed binding mode of compound **6** to N-terminal-Hsp90α.

while it shows the significant rearrangement in the structures of **1** and **4**, resulting in 'semi-open' and 'open' conformations, respectively (Fig. 3). Such a conformational flexibility of this part of the molecule was reported previously.[17] It would be possible to exploit a hydrophobic pocket created by the formation of α-helix in the structure of **3** to design more potent inhibitors, but we focused on **1** and **4**, as the shapes of the binding pocket of **1** and **4** are more similar to each other and therefore it was expected to be more straightforward to design new inhibitors by merging the structural information on **1** and **4**. In addition, the slower dissociation of **4** with 0.10/s when compared to **3** (>1/s), was preferred as an initial hit (data not shown). A fast dissociation observed for **3** suggested that the formation of α-helix in the residues Ile110-Gly114 would not be a rate-limiting step, but that this portion would be in the very rapid equilibrium between the different conformations.

In order to search for additional interaction points for increasing potencies of **4**, the binding site of the obtained X-ray structure, was analyzed using the program GRID (Molecular Discovery, http://moldiscovery.com).[18,19] A regular grid was built over the rectangular box defined by the size of compound **4** as found in the complex structure of **4** and Hsp90. Then for each grid, the interaction energy of the DRY probe, which represents steric and hydrophobic interactions, was computed using the GRID force field. The GRID descriptor thus calculated revealed the small hydrophobic space formed by Leu107 and Phe138 close to the tricyclic group of **4**, which could be filled with methyl group or halogen atom (Fig. 4a). In fact, model compounds **5**–**7**, showed that an introduction of methyl group or chlorine atom at the *ortho*-position of the phenyl ring led to a remarkable improvement of the affinity over the non-substituted form, **5**, with the K_d values 11 or seven times smaller than that of **5**, respectively (Fig. 4b). Concomitantly, LEI was increased from 0.39 to 0.45 or 0.44. The X-ray structure of **7** confirmed that the introduced chloro atom occupies the small hydrophobic pocket as expected (Fig. 4c).[16]

Combining all the information obtained together, we designed and synthesized the 'hybrid' compound CH5015765 which has 2-aminotriazine as a core and an *S*-methyl group at the C-4 position and an *ortho*-Cl-tricyclic group at the C-6 position (Fig. 5a). Remarkably, this compound showed significantly improved binding affinity over the hit compounds from fragment screening and virtual screening, with a K_d value of 3.4 nM and LEI of as high as 0.50. No significant change was found for the inhibitory activity of the ATPase assay, but this was due to an inherent low sensitivity of the assay system. The binding mode of the compound was not altered, as revealed by the X-ray structure analysis (Fig. 5b).[16] In addition, in vitro cell growth inhibition (CGI) assay using HCT116 cells showed that this compound had CGI activities with an IC_{50} value of 0.46 μM. In order to confirm that the observed CGI was due to the suppression of Hsp90 and not due to the general toxic effect, the down-regulation of the Hsp90 client proteins, Her2, Raf1 and pERK, was measured at 0.5, 5, and 50 μM of the compound (Fig. 5c). The analysis of the HCT116 cells treated with the inhibitor demonstrated that such down-regulation was indeed induced in a manner dependent on the inhibitor concentrations. PK profile of this compound indicated some oral bioavailability in mouse (4.5%), despite the high plasma clearance of 19.5 mL/min/kg, which encouraged us to measure in vivo antitumor activity of this compound (Fig. 5d). Remarkably, when CH5015765 was administered orally to mice, it exhibited 54% inhibition of tumor volume at a dose of 400 mg/kg in a human stomach cancer NCI-N87 xenograft model, without any loss of body weight (Fig. 5e.).

Noteworthy is that, when LEI of the inhibitors is plotted against molecular weight, LEI is actually not only maintained, but rather improved over the course of the modification (Fig. 6). This was uncommon as, in general, LEI decreases or, at most, stays at a comparable value as the molecular weight of compounds increases during compound optimization.[20] This clearly demonstrates that

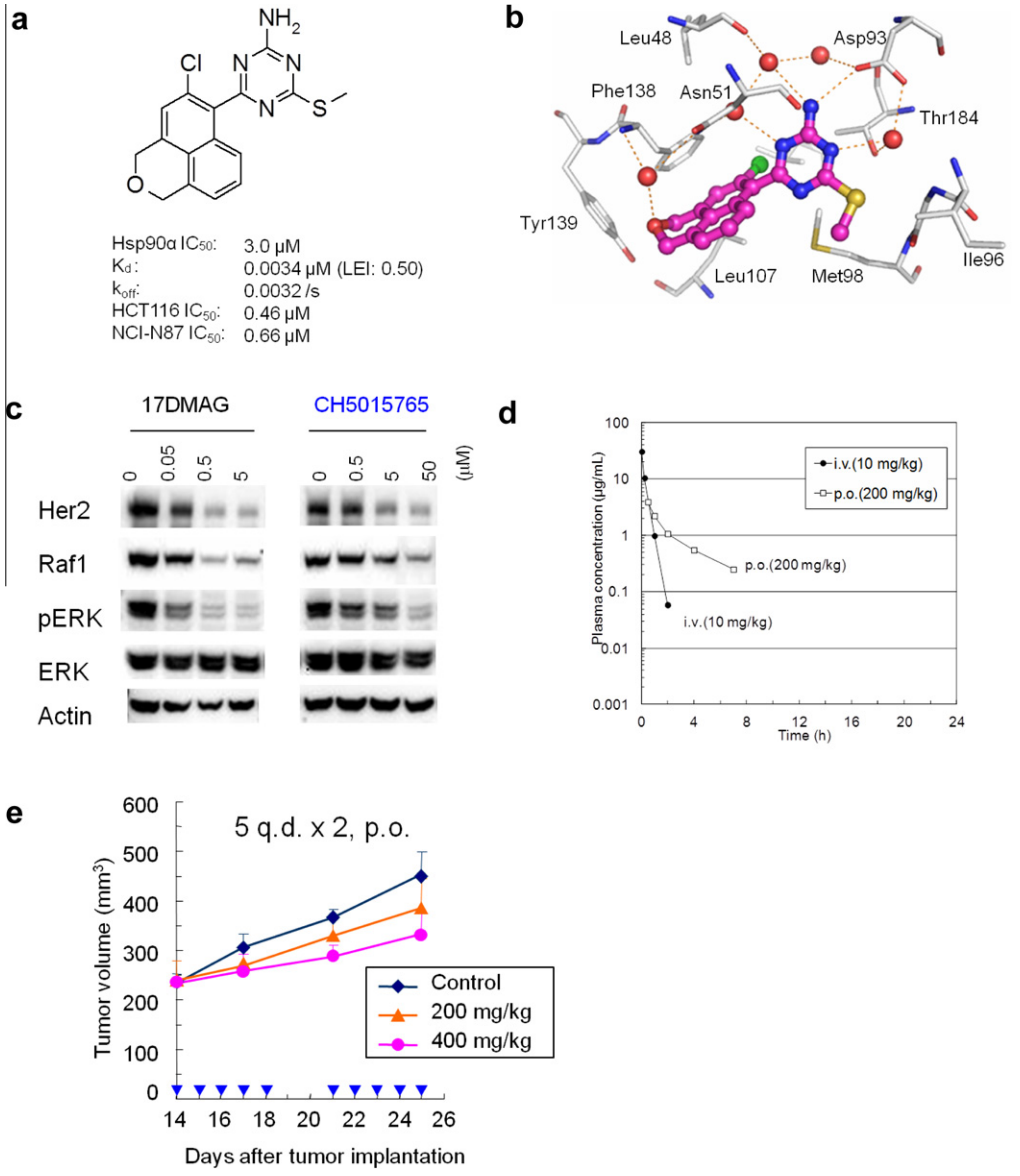

Figure 5. Biological activities of CH5015765. (a) Chemical structure of CH5015765 and its in vitro activities. (b) Binding mode of CH5015765 in Hsp90. (c) Effects of CH5015765 on expression of Her2, Raf1, pERK and ERK. Actin was used as a loading control. (d) PK profile of CH5015765 in mouse. (e) In vivo antitumor activity of CH5015765 in human stomach cancer NCI-N87 xenograft mouse model.

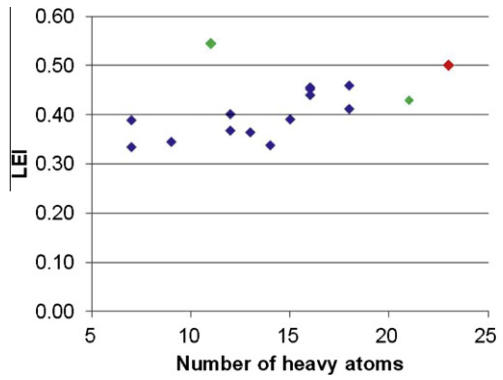

Figure 6. A plot of LEI values to number of heavy atoms for the series of Hsp90 inhibitors in this study. Symbols corresponding to fragment hit **1** and virtual screening hit **4** are colored in green; CH5015765 in red.

our combined approach was extremely robust in efficiently generating a good lead compound.

In summary, we discovered a new class of orally available Hsp90 inhibitor with in vivo antitumor activity, by combining the information derived from the hits from the two types of screening and molecular modeling/X-ray analysis. The information from the screenings was more directly used to design the new inhibitor in our study. This combined and direct use of the information from the different approaches was a key for success in quickly developing the potent inhibitor. Further modification of CH5015165 to improve its physicochemical property and oral bioavailability, has been carried out and the work will be reported elsewhere as a separate paper.

Acknowledgments

We thank Kenichi Kawasaki, Susumu Komiyama, Kazuhiro Ohara, Yasue Nagata, Osamu Kondoh, Kiyoaki Sakata, Toshikazu Yamazaki and all people who contributed to this work.

Supplementary data

Supplementary data associated with this article can be found, in the online version, at doi:10.1016/j.bmcl.2011.08.001.

References and notes

1. Duerfeldt, A. S.; Blagg, B. S. J. *Bioorg. Med. Chem. Lett.* **2010**, *20*, 4983.
2. Whitesell, L.; Mimnaugh, E. G.; Costa, B. De.; Myers, C. E.; Neckers, L. M. *Proc. Natl. Acad. Sci. U.S.A.* **1994**, *91*, 8324.
3. Taldone, T.; Gozman, A.; Maharaj, R.; Chiosis, G. *Curr. Opin. Pharmacol.* **2008**, *8*, 370.
4. Porter, J. R.; Fritz, C. C.; Depew, K. M. *Curr. Opin. Chem. Biol.* **2010**, *14*, 412.
5. Murray, C. W.; Carr, M. G.; Callaghan, O.; Chessari, G.; Congreve, M.; Cowan, S.; Coyle, J. E.; Downharm, R.; Figueroa, E.; Frederickson, M.; Graham, B.; McMenamin, R.; O'Brien, M. A.; Patel, S.; Phillips, T. R.; Williams, G.; Woodhead, A. J.; Woolford, A. J. *J. Med. Chem.* **2010**, *53*, 5942.
6. Brough, P. A.; Barril, X.; Borgognoni, J.; Chene, P.; Davies, N. G.; Davis, B.; Drysdale, M. J.; Dymock, B.; Eccles, S. A.; Garcia-Echeverria, C.; Fromont, C.; Hayes, A.; Hubbard, R. E.; Jordan, A. M.; Jensen, M. R.; Massey, A.; Merrett, A.; Padfield, A.; Parsons, R.; Radimerski, T.; Raynaud, F. I.; Robertson, A.; Roughley, S. D.; Schoepfer, J.; Simmonite, H.; Sharp, S. Y.; Surgenor, A.; Valenti, M.; Walls, S.; Webb, P.; Wood, M.; Workman, P.; Wright, L. *J. Med. Chem.* **2009**, *52*, 4794.
7. Stebbins, C. E.; Russo, A. A.; Schneider, C.; Rosen, N.; Hartl, F. U.; Pavletich, N. P. *Cell* **1997**, *89*, 239.
8. Obermann, W. M. J.; Sondermann, H.; Russo, A. A.; Pavletich, N. P.; Hartl, U. H. *J. Cell. Biol.* **1998**, *143*, 901.
9. Miura, T.; Klaus, W.; Ross, A.; Sakata, K.; Masubuchi, M.; Senn, H. *Eur. J. Biochem.* **2001**, *268*, 4833.
10. Shuker, S. B.; Hajduk, P. J.; Meadows, R. P.; Fesik, S. W. *Science* **1996**, *274*, 1531.
11. Hsp90α ATPase assay was performed in a 96-well plate. 100 μl of the reaction mixture containing 30–100 μg full-length Hsp90α and 10 mM ATP in 50 mM tris(hydroxymethyl)aminomethane–HCl, pH 7.6, 10 mM KCl, 5 mM $MgCl_2$, was incubated for 1 h at 37 °C. Tested compounds were prepared in DMSO as 100× stock and added to the reaction mixture at a final DMSO concentration of 1%. After the incubation, the amount of inorganic free phosphate produced by the ATPase activity of Hsp90α, was quantitated by the addition of 100 μl malachite green solution and the subsequent measurement of the absorbance at 655 nM using a microplate reader.
12. Hopkins, A. L.; Groom, C. R.; Alex, A. *Drug Discovery Today* **2004**, *9*, 430.
13. Rarey, M.; Kramer, B.; Lengauer, T.; Klebe, G. *J. Mol. Biol.* **1996**, *261*, 470.
14. Gasteiger, J.; Rudolph, C.; Sadowski, J. *Tetrahedron Comp. Method* **1990**, *3*, 537.
15. Crystals were grown by the hanging drop vapor diffusion technique. Drops were prepared by mixing 1 μl of 10–20 mg/mL protein and 1 mM inhibitor solution with 1 μl of reservoir solution, containing 18–27% (w/v) Polyethyleneglycol 3350, 0.2–0.4 M $MgCl_2$, 0.1 M Tris–Cl (pH 8.0), and were incubated at 277 K against 400 μl of the reservoirs for 1–2 weeks. X-ray diffraction datasets were collected at the beamlines of BL-6B and AR-NW12A in Photon Factory, KEK and X10SA in Swiss Light Source.
16. The atomic coordinates and structure factors for the N-terminal domain of Hsp90α in complex with **1**, **3**, **4**, **7**, and CH5015765, have been deposited in the Protein Data Bank under accession code, 3B24, 3B25, 3B26, 3B27, and 3B28, respectively.
17. Wright, L.; Barril, X.; Dymock, B.; Sheridan, L.; Surgenor, A.; Besweick, M.; Drysdale, M.; Collier, A.; Massey, A.; Davies, N.; Fink, A.; Fromont, C.; Aherne, W.; Boxall, K.; Sharp, S.; Workman, P.; Hubbard, P. E. *Chem. Biol.* **2004**, *11*, 775.
18. Goodford, P. J. *J. Med. Chem.* **1985**, *28*, 849.
19. Boobbyer, D. N.; Goodford, P. J.; McWhinnie, P. M.; Wade, R. C. *J. Med. Chem.* **1989**, *32*, 1083.
20. Reynolds, C. H.; Tounge, B. A.; Bembenek, S. C. *J. Med. Chem.* **2008**, *51*, 2432.